Current Research in Structural Biology 6 (2023) 100110

Contents lists available at ScienceDirect

Current Research in Structural Biology

journal homepage: www.journals.elsevier.com/current-research-in-structural-biology

Research Article

Novel peptide inhibitors targeting CD40 and CD40L interaction: A potential for atherosclerosis therapy

Kundan Solanki [a,1], Ashutosh Kumar [b,1], Mohd Shahnawaz Khan [c], Subramani Karthikeyan [d], Rajat Atre [a], Kam Y.J. Zhang [b], Evgeny Bezsonov [e,f,g], Alexander G. Obukhov [h,i,**], Mirza S. Baig [a,*]

[a] Department of Biosciences and Biomedical Engineering (BSBE), Indian Institute of Technology Indore (IITI), Simrol, Indore, 453552, India
[b] Laboratory for Structural Bioinformatics, Center for Biosystems Dynamics Research, RIKEN, Tsurumi, Yokohama, Kanagawa, Japan
[c] Department of Biochemistry, College of Science, King Saud University, Riyadh, 11451, Saudi Arabia
[d] Centre for Healthcare Advancement, Innovation and Research, Vellore Institute of Technology University, Chennai Campus, Chennai, 600127, India
[e] Laboratory of Angiopathology, Institute of General Pathology and Pathophysiology, 8 Baltiiskaya Street, 125315, Moscow, Russia
[f] Laboratory of Cellular and Molecular Pathology of Cardiovascular System, Avtsyn Research Institute of Human Morphology of Federal State Budgetary Scientific Institution "Petrovsky National Research Centre of Surgery", 3 Tsyurupa Street, 117418, Moscow, Russia
[g] Department of Biology and General Genetics, I.M. Sechenov First Moscow State Medical University (Sechenov University), 8 Izmailovsky Boulevard, 105043, Moscow, Russia
[h] Department of Anatomy, Cell Biology & Physiology, Indiana University School of Medicine, Indianapolis, IN, 46202, USA
[i] Stark Neurosciences Research Institute, Indiana University School of Medicine, Indianapolis, IN, 46202, USA

ARTICLE INFO

Handling editor: A Wlodawer

Keywords:
Atherosclerosis
CD40 recepto
CD40L
Peptidomimetics
In-silico screening

ABSTRACT

Atherosclerosis is a chronic inflammatory disease characterized by plaque build-up in the arteries, leading to the obstruction of blood flow. Macrophages are the primary immune cells found in the atherosclerotic lesions and are directly involved in atherosclerosis progression. Macrophages are derived from extravasating blood monocytes. The monocytic CD40 receptor is important for monocyte recruitment on the endothelium expressing the CD40 ligand (CD40L). Thus, targeting monocyte/macrophage interaction with the endothelium by inhibiting CD40-CD40L interaction may be a promising strategy for attenuating atherosclerosis. Monoclonal antibodies have been used against this target but shows various complications. We used an array of computer-aided drug discovery tools and molecular docking approaches to design a therapeutic inhibitory peptide that could efficiently bind to the critical residues (82Y, 84D, and 86N) on the CD40 receptor essential for the receptor's binding to CD40L. The initial screen identified a parent peptide with a high binding affinity to CD40, but the peptide exhibited a positive hepatotoxicity score. We then designed several novel peptidomimetic derivatives with higher binding affinities to CD40, good physicochemical properties, and negative hepatotoxicity as compared to the parent peptide. Furthermore, we conducted molecular dynamics simulations for both the apo and complexed forms of the receptor with ligand, and screened peptides to evaluate their stability. The designed peptidomimetic derivatives are promising therapeutics targeting the CD40-CD40L interaction and may potentially be used to attenuate atherosclerosis.

1. Introduction

Atherosclerosis is a chronic inflammatory disease in which plaque build-up due to the deposition of cholesterol, lipids, and fats as well as extravasation of immune cells in the arteries lead to an obstruction of blood flow. Atherosclerosis is a major cause of cardiovascular diseases (CVD) and is a risk factor for myocardial infarction (MI) and ischemic stroke (Lusis, 2000). Pharmacological treatments such as lipid-lowering therapies, anti-hypertensive agents, and anti-platelets drugs reduce the risk of CVD, but atherosclerosis-related complications remain persistent

* Corresponding author.
** Corresponding author. Department of Anatomy, Cell Biology & Physiology, Indiana University School of Medicine, Indianapolis, IN, 46202, USA.
E-mail addresses: aobukhov@iu.edu (A.G. Obukhov), msb.iit@iiti.ac.in (M.S. Baig).
[1] Equal contribution: Kundan Solanki, Ashutosh Kumar.

https://doi.org/10.1016/j.crstbi.2023.100110
Received 24 July 2023; Received in revised form 25 October 2023; Accepted 26 October 2023
Available online 14 November 2023

worldwide (Aday and Ridker, 2019; Peikert et al., 2020). Thus far, several clinical trials have focused on targeting inflammatory molecules implicated in the progression of atherosclerosis (Ridker et al., 2017, 2019; Tardif et al., 2019). Another strategy is to inhibit inflammation and/or to modulate the immune checkpoint proteins, promoting inflammation (Kusters et al., 2018). The CD40-CD40L dyad is an important immune checkpoint protein complex that is expressed on major immune cells, and its activation leads to the progression of atherosclerosis (Bosmans et al., 2021; Lacy et al., 2021).

CD40L plays an important role in the pathogenesis of atherosclerosis (Lutgens et al., 2007). Cells such as myeloid and lymphoid cells, platelets, endothelial cells and vascular smooth muscle cells (VSMCs) are known to express CD40L on their surfaces (Mach et al., 1997). CD40L expression is primarily found on T-cells and platelets in atherosclerosis (Michel et al., 2017). CD40L present on these cells would bind to CD40 receptor expressed on antigen presenting cells (APCs) to amplify the signaling (Quezada et al., 2004). Apart from CD40, CD40L also bind to other co-stimulatory receptor present on the cell surface to activate the inflammation response (Lacy et al., 2021). One of the major roles of CD40-CD40L interaction is the recruitment of monocytes and other immune cells to the site of inflammation during the initial phase of plaque formation. The endothelial cells are activated when the monocytic CD40 receptor binds the endothelial CD40L. This enhances the expression of cell adhesion molecules (CAMs) such as vascular cell adhesion molecule (VCAM)-1, intercellular cell adhesion molecule (ICAM)-1 and E-selectin on the endothelium (Kotowicz et al., 2000). Remarkably, high Ox-LDL levels drive the expression of the CD40 receptor on monocytes/macrophages and CD40L on the endothelial cell, further enhancing the expression of CAMs on the endothelial cells and facilitating the recruitment and transmigration of monocytes into the arterial intima, critical steps of atherosclerosis progression (Roy et al., 2021). Migration of monocytes into the intima leads to their differentiation into macrophages. These macrophages secrete various pro-inflammatory molecules and further enhance the inflammation process. Thus, inhibition of the CD40-CD40L interaction may be important for preventing chronic consequences of atherosclerosis. Indeed, studies have found that genetic or antibody-mediated inhibition of CD40 or CD40L reduces the inflammatory cell number within the plaque with a subsequent decrease in the lesion size and enhanced plaque stability (Engel et al., 2009; Lutgens et al., 2000; Schonbeck et al., 2000). CD40-TRAF6 interaction is present downstream of CD40-40L interaction (Lutgens et al., 2010). Inhibition of CD40-TRAF6 with TRAF-STOP inhibitors have shown promising results (Seijkens et al., 2018). Multiple antibodies have been developed to target the CD40-CD40L interaction (Croft et al., 2013), but the strong immune response against the antibodies and thromboembolic complications limit their usage. (Leader et al., 2008). Thus, it is important to search for better therapeutic strategies that would have enhanced efficacy with limited side effects.

In the past few years, peptides and peptidomimetics have emerged as promising candidates to treat various diseases by modulating protein-protein interactions (PPIs) (Recio et al., 2016; Vagner et al., 2008). There are now peptides that successfully target certain biologically important protein complexes, such as transcription factors, which are traditionally considered as undruggable targets for small molecules because of their complex architecture and stability (Seo et al., 2011). However, peptides possess certain characteristics that limit their usage as therapeutic candidates, such as low metabolic stability towards proteolysis in the gastrointestinal tract and serum, their poor absorption after oral ingestion, and their rapid excretion through the liver and kidneys (Recio et al., 2016). Hence, advancements are necessary to meet the increased therapeutic demands. Recent technological advances in formulation, delivery, and chemistry have driven the focus of drug discovery teams toward peptidomimetics (Antosova et al., 2009; Audie and Boyd, 2010; Timmerman et al., 2005). Peptidomimetics are compounds whose essential elements (or pharmacophore) mimic a peptide or protein in their 3D space and which primarily tend to retain the ability to interact with the specified biological target and impart the same biological effect. Certain limitations of peptides can be compensated through creating peptidomimetics with increased stability against proteolysis, receptor selectivity or potency, among others. Hence, peptidomimetics have a great potential in drug discovery (Vagner et al., 2008). Also, designing/deriving compounds that contain the same backbone elements as peptidomimetic with few modifications in the side chains, which can increase the affinity of the compound with the target, can be a better therapeutic strategy against the target molecule (Li Petri et al., 2022).

Identification of the critical residues on the target protein is important for designing the molecules limiting the protein-protein interaction. *In-vitro* studies have identified three critical residues on the CD40 receptor (Y82, D84, and N86) having a key role in its interaction with CD40L (Bajorath et al., 1995). In this study, we focused on designing peptides that may bind to these critical residues. Furthermore, we derived promising peptidomimetics and their derivatives with increased affinity to the CD40 receptor and improved physicochemical properties.

2. Methods

2.1. Analyses of CD40-40L interface and docking of CD40-CD40L

The crystal structure of CD40-CD40L interaction (**PDB ID:** 3QD6) was retrieved from RCSB Protein Data Bank (https://www.rcsb.org). The crystal structure was analysed by the X-Ray diffraction method with a resolution of 3.5 Å. The complex contains a total of 4 CD40 receptor chains (Chain R, S, T, and U) interacting with 6 CD40L chains (Chain A, B, C, D, E, and F) in a ratio of 2:3 of receptor: ligand complex (An et al., 2011). The complex was downloaded as a PDB file, and the monomer of the CD40 receptor (Chain S) interacting with the CD40L monomer (Chain C) was taken for further interaction studies. 4 Å interacting residues between the complex were analysed in UCSF Chimera (Pettersen et al., 2004). Also, the individual monomers of both the receptor and the ligand were structurally minimized using Amber ff14SB (Maier et al., 2015) in the UCSF Chimera, and site-specific docking was done in PyDockWEB (https://life.bsc.es/pid/pydockweb) (Jimenez-Garcia et al., 2013) providing the 4 Å interacting residues between the complex.

2.2. In-silico mutational analysis of CD40-40L interaction

As the *in-vitro* mutational study had identified Y82, D84, and N86 as a critical residue on the CD40 receptor mediating the interaction with the ligand, we wanted to further confirm the result through *in-silico* study. Individual mutations on the CD40 receptor (Y82, D84, and N86) were done using the Rotamer option in UCSF Chimera (Pettersen et al., 2004), replacing key residues with alanine one at a time. The structure was then minimized using Amber ff14SB (Maier et al., 2015) in Chimera and docked with the CD40L (Chain C) in HDOCK (http://hdock.phys.hust.edu.cn/) (Yan et al., 2020) providing the 4 Å interacting residues between the complex. Also, the triple mutations were done in CD40 before docking with wild type CD40L to compare the change in binding affinity with the individual mutations. Similar strategy was employed on CD40L by mutating the residues K143 and Y145 individually and by performing the double mutations (Chain C) and docked to CD40 in HDOCK (http://hdock.phys.hust.edu.cn/) (Yan et al., 2020).

2.3. The design and docking of the peptide

Four-amino acid peptide (*p-KGYY*) was designed against the critical residues on the receptor to block the receptor-ligand interaction. Stretch from residues 143–146 on the CD40L was used to design the peptide using the "*Build structure*" option in UCSF Chimera (Pettersen et al., 2004). The designed peptide was then minimized using Amber ff14SB and docked with the CD40-receptor (Chain S) in PyDockWEB

(Jimenez-Garcia et al., 2013) and ZDOCK (Pierce et al., 2014). 4 Å interacting residues between the complex were analysed in UCSF Chimera to find the critical residue(s) on the receptor involved in the binding with the peptide. Further, physicochemical and ADMET analyses of the peptide were done using the pkCSM server (https://biosig.lab.uq.edu.au/pkcsm/) (Pires et al., 2015). pkCSM uses graph-based signatures of the compounds to analyse the ADMET properties of the compounds by comparing them with the *in-vitro* data available on the server. The SMILES file of the compounds was generated on the pepSMI server (https://www.novoprolabs.com/tools/convert-peptide-to-smiles-string) and then analysed on the pkCSM server to optimize its ADMET properties.

2.4. The docking of peptidomimetic with the receptor

To address the limitations of the designed peptide, peptidomimetics that mimic the structure as well as the pharmacophore of the designed peptide were searched on the pep:MMs:MIMIC server (http://mms.dsfarm.unipd.it/pepMMsMIMIC/) (Floris et al., 2011). pep:MMs:MIMIC is a server in which the 3D-similarity search of the peptides is possible among 3.9 million commercial compounds in the MMsINC database (http://mms.dsfarm.unipd.it/MMsINC/search/) (Masciocchi et al., 2009). Side chains of the lysine and tyrosine residue on the peptide were selected and fingerprint-based filtering of shape similarity and pharmacophoric similarity-based methods were used to provide the top 200 compounds from the database. All the compounds were downloaded in the 3D SDF format and docked to the CD40 receptor (Chain S; PDB 3QD6). Two docking platforms were used: AutoDock Vina (v1.2.0) (Eberhardt et al., 2021; Trott and Olson, 2010) and the Glide module of the Schrodinger suite (Friesner et al., 2004). Preparation of the receptor for docking in AutoDock Vina (v1.2.0) was done by adding polar hydrogen bonds followed by the addition of Kolmann charges in AutoDock 4.2.6 (Morris et al., 2009). A grid box was generated around the receptor covering the whole receptor molecule. For docking in Schrodinger, the protein preparation wizard of the Schrodinger suite (Sastry et al., 2013; Schrodinger, 2021b) was used in which missing hydrogens were added, followed by the removal of heteroatoms and water molecules. The structure was then refined and optimized at pH 7.0 using PROPKA (Olsson et al., 2011), followed by minimization using OPLS4 force-field (Lu et al., 2021). The receptor grid was generated by selecting the 4 Å residues on the CD40 receptor interacting with the ligand in the crystal structure. The docked compounds were shortlisted based on the interaction of the peptidomimetic with all three critical residues (Y82, D84, and N86) in AutoDock Vina (v1.2.0) and Schrodinger. Further, physicochemical and ADMET analyses of the lead compounds were done on the pkCSM server (Pires et al., 2015).

2.5. The docking of peptidomimetic derivative

As the derived peptidomimetic had limitations in its ADMET property, we sought to find the derivatives of the lead compounds which can increase the binding affinity with the receptor as well as have good ADMET properties. A structural similarity search of the lead compounds was done in PubChem (https://pubchem.ncbi.nlm.nih.gov/) by uploading the SMILES ID of the peptidomimetic structure. The resulting compounds were downloaded as 2D SDF and converted to 3D by the LigPrep module of the Schrodinger suite (Schrodinger, 2021a). 3D SDF files were converted into pdbqt in Open Babel (O'Boyle et al., 2011) and docked with the CD40 receptor (Chain S) in AutoDock Vina (v1.2.0) (Eberhardt et al., 2021; Trott and Olson, 2010). Compounds were then screened accordingly through their interaction with the three critical residues on the receptor. The shortlisted compounds were further docked in Glide (Friesner et al., 2004) to find a similar interaction with the receptor. Physicochemical analysis of the top compounds in both platforms was done in the pkCSM server (Pires et al., 2015) to find the compound(s) with good ADMET properties.

2.6. Molecular dynamics simulation

Further, to understand the stability of the screened peptide (p-KGYY)- CD40 receptor complex, all the apo and complex forms were subjected to molecular dynamics simulation using Gromacs 2020.4 software (Abraham et al., 2015; Van Der Spoel et al., 2005). The input structures were prepared with Charmm 36 (MacKerell et al., 2000; Vanommeslaeghe et al., 2010) force field using CHARMM GUI online input generator (Gao et al., 2021; Jo et al., 2008; Lee et al., 2016). Cubic boxes of 10 $Å^3$ were kept as periodic boundary condition using supramolecular centre of mass of the protein. TIP3P water model was used as a buffer to neutralize the Ewald charge distribution of the solvated structure. The protein structures were minimized energetically and underwent two stage equilibration process with NVT and NPT ensembles. Then, the simulation was carried out for a period of 100ns. The results were analysed using VMD software.

3. Results

3.1. Structural analysis and docking of the CD40 receptor with the CD40 ligand

To validate our computer modelling approach, we first analysed the crystal structure of the CD40-CD40L protein complex (RCSB: PDB 3QD6) to deduce the critical residues involved in the protein-protein interactions. The protein-protein interface of the CD40 receptor (Chain S) and CD40 ligand (Chain C) was scrutinized using UCSF Chimera (Pettersen et al., 2004) to identify all residues which are found within the range of ionic and hydrogen bonding interactions of 4 Å (Fig. 1A and B). Our analysis confirmed a previous study finding that there are three critical residues on the CD40 receptor (Y82, D84, and N86) and two critical residues on the CD40 ligand (K143 and Y145) contributing to the protein-protein interactions within the CD40R-CD40L protein complex (Bajorath et al., 1995). The monomeric chains of the CD40 receptor (Chain S) and ligand (Chain C) were also docked using PyDockWEB (Jimenez-Garcia et al., 2013) and then analysed for the 4 Å range residues within the CD40R-CD40L complex. The docking results again showed the involvement of similar residues in mediating CD40R-CD40L interactions (Fig. 2).

3.2. In silico mutational analysis of the CD40 receptor and CD40L

To further decipher the importance of the critical residues on the receptor (Y82, D84, and N86) and the ligand (K143 and Y145), *in-silico* point mutational analysis was performed during which the critical residues on the CD40 receptor were individually replaced with alanine. Additionally, we created the CD40 receptor mutant in which all three critical residues were replaced with alanine. We then docked each *in-silico* created mutant of the CD40 receptor with the CD40 ligand using the HDOCK server (http://hdock.phys.hust.edu.cn/) (Yan et al., 2020). Control docking of the wild type CD40 receptor (without mutations) with the CD40 ligand was performed to compare the docking scores among the wild type and mutated complexes. The results showed decreases in the docking scores of the individually mutated CD40 receptors compared to the wild type CD40 receptor used as a control, with the highest decrease in the mutated CD40 receptor where all three critical residues were replaced with alanine (Fig. 3). Similarly, the critical residues on the CD40 ligand (K143 and Y145) were also mutated individually or together and then docked with the CD40 receptor using HDOCK (Yan et al., 2020). The result again showed decreases in the binding affinity in the mutated structures compared to the control, with the highest decrease found in the combined mutated structures (Fig. 4).

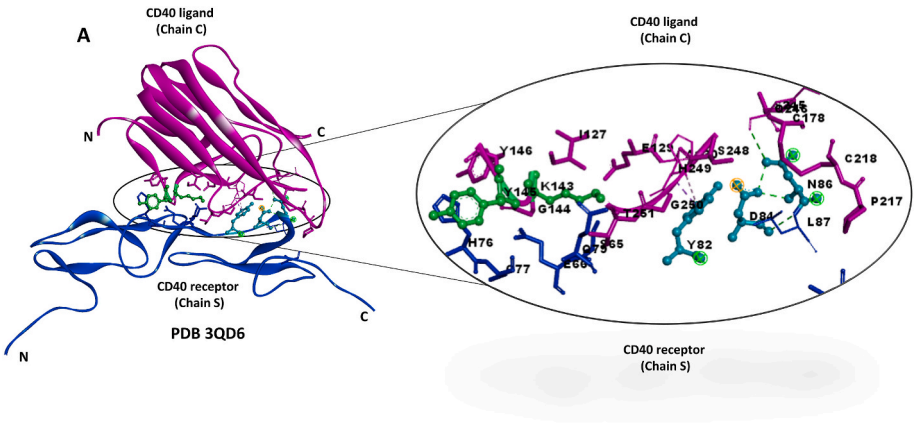

B

4Å residues	
CD40 receptor	**CD40 ligand**
65, 66, 76, 77, 79, **82**, **84**, **86**, 87, 119	127, 129, 130, **143**, 144, **145**, 146, 178, 217, 218, 245, 246, 248, 249, 250, 251

Fig. 1. Analysis of the crystal structure of CD40-CD40L (PDB 3QD6): A.) Schematic representation of the CD40 receptor (Chain S) interacting with CD40L (Chain C). 4 Å interacting residues between the complex have been highlighted in the circle. **B)** Table showing 4 Å interacting residues between the CD40 receptor (Chain S) and CD40L (Chain C). Residues in bold indicate critical residues in the receptor and the ligand. CD40 is highlighted in blue, and CD40L is highlighted in pink. (For interpretation of the references to colour in this figure legend, the reader is referred to the Web version of this article.)

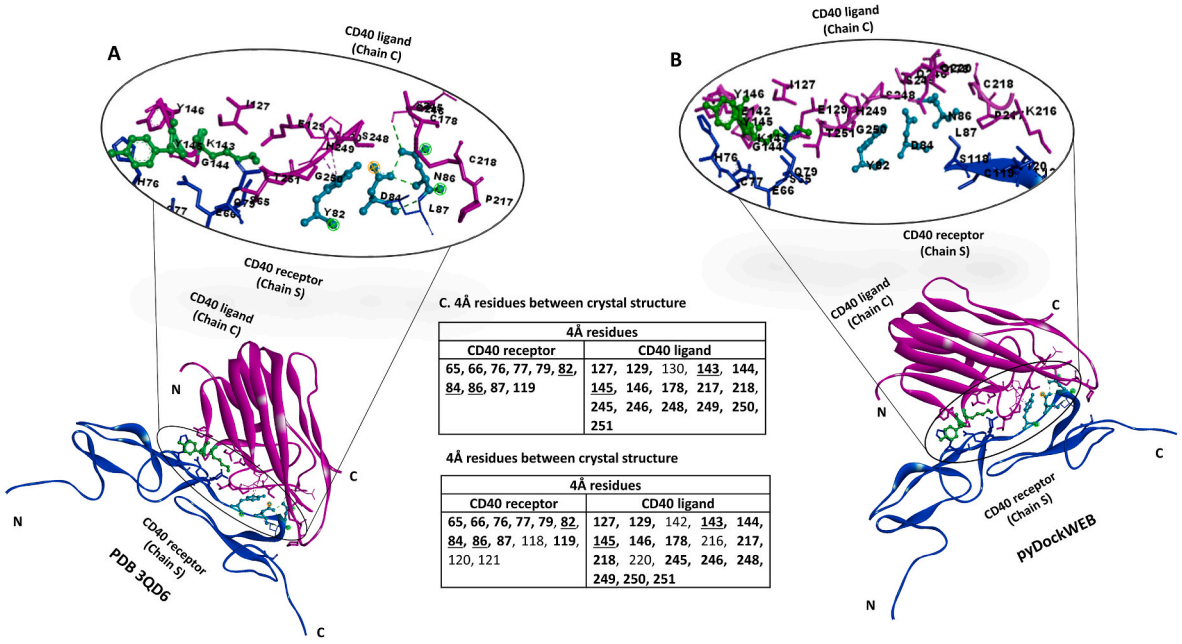

C. 4Å residues between crystal structure

4Å residues	
CD40 receptor	**CD40 ligand**
65, 66, 76, 77, 79, 82, 84, 86, 87, 119	**127, 129,** 130, **143, 144, 145, 146, 178, 217, 218, 245, 246, 248, 249, 250, 251**

4Å residues between crystal structure

4Å residues	
CD40 receptor	**CD40 ligand**
65, 66, 76, 77, 79, 82, 84, 86, 87, 118, **119,** 120, 121	**127, 129,** 142, **143, 144, 145, 146, 178,** 216, **217, 218,** 220, **245, 246, 248, 249, 250, 251**

Fig. 2. Comparison of the crystal structure and the docked structure: A.) Crystal structure of CD40 (Chain S) and CD40L (Chain C) along with 4 Å residues highlighted in the circle. **B.)** Docking of CD40 (Chain S) and CD40L (Chain C) in PyDockWEB along with 4 Å residues highlighted in the circle. **C.)** Table showing 4 Å interacting residues between crystal and docked structures of CD40-CD40L. Matching residues between the crystal and the docked structures are highlighted in bold and critical residues (82Y, 84D, and 86N) are underlined. CD40 is highlighted in blue, and CD40L is highlighted in pink. (For interpretation of the references to colour in this figure legend, the reader is referred to the Web version of this article.)

3.3. Designing of the inhibitory peptide and its docking to the CD40 receptor

Since the interaction of CD40 and CD40L is strongly implicated in atherogenesis, we next set out to design a small therapeutic inhibitory peptide capable of preventing the CD40-CD40L complex formation. A continuous stretch of residues in the CD40 ligand (143–146), critical for the interaction with CD40, was used as a template to design the therapeutic inhibitory peptide structure. The peptide (p-KGYY) was designed using UCSF Chimera (Pettersen et al., 2004) and then docked to the CD40 receptor (PDB 3QD6; Chain S) using PyDockWEB (Jimenez-Garcia et al., 2013) and ZDOCK (Pierce et al., 2014). The residues within the 4 Å range in the docked peptide-CD40 complex were analysed and compared with the interacting residues in the crystal structure of the CD40-CD40L complex. We found that the peptide-CD40 interface was very similar to that of the equivalent stretch in the CD40-CD40L crystal structure (Fig. 5). However, while conducting the physicochemical and ADMET analyses of the peptide using the pkCSM server (Pires et al.,

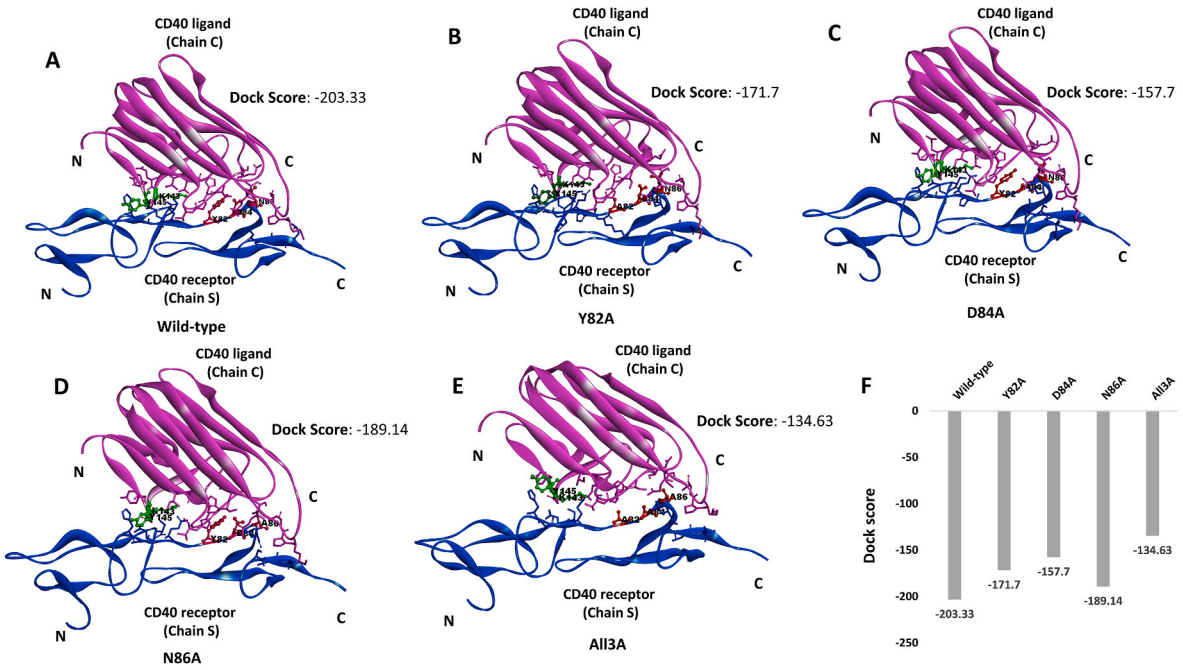

Fig. 3. Effect of mutation(s) on the critical residue(s) on the receptor binding with the ligand: Figure showing the docking of CD40 (Chain S) and CD40L (Chain C) with individual mutation(s) along with the dock scores in HDOCK. **A.)** Wild-type (no mutation). **B.)** Y82A. **C.)** D84A. **D.)** N86A. **E.)** All three mutations. **F.)** Graph comparing the dock scores between all mutations. Residues 82, 84, and 86 in the receptor are highlighted in red, and residues 143 and 145 in the ligand have been highlighted in green. CD40 is highlighted in blue, and CD40L is highlighted in pink. (For interpretation of the references to colour in this figure legend, the reader is referred to the Web version of this article.)

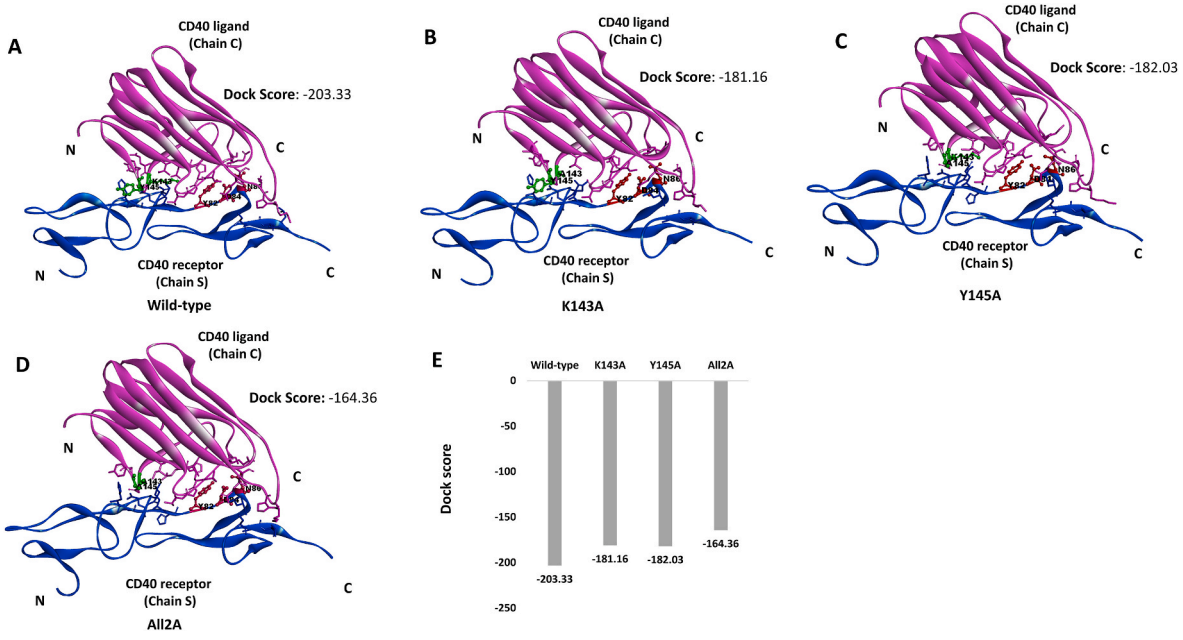

Fig. 4. Effect of mutation(s) on the critical residue(s) on the binding of CD40L with CD40: Figure showing the docking of CD40 (Chain S) and CD40L (Chain C) with individual mutation(s) along with the dock scores in HDOCK. **A.)** Wild-type (no mutation). **B.)** K143A. **C.)** Y145A. **D.)** Both the mutations. **E.)** Graph comparing the dock scores between all the mutations. Residues 82, 84, and 86 in the receptor are highlighted in red, and residues 143 and 145 in the ligand are highlighted in green. CD40 is highlighted in blue, and CD40L is highlighted in pink. (For interpretation of the references to colour in this figure legend, the reader is referred to the Web version of this article.)

2015), we found that the designed peptide may exhibit hepatotoxicity (Table 1). These urged us to search for a better therapeutic molecule with a safer profile.

3.4. Peptidomimetics as a therapeutic strategy to block CD40-CD40L interactions

To address the limitations of the derived peptide structure, peptidomimetics were used as an alternative therapeutic strategy. The peptidomimetic pep:MMs:MIMIC server (http://mms.dsfarm.unipd.it/pep

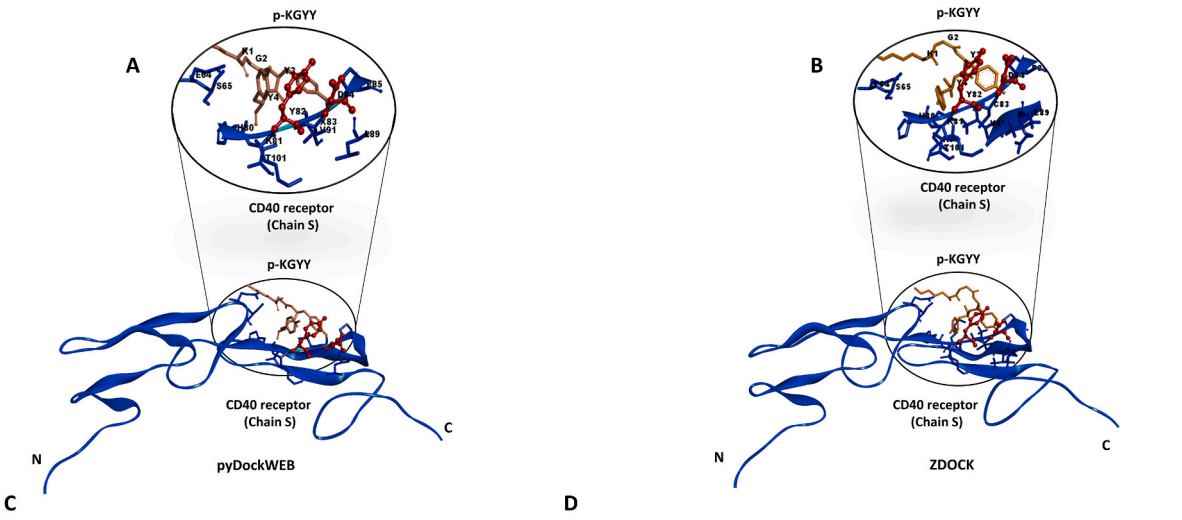

C

4Å residues	
CD40 receptor	CD40 ligand
65, 66, 76, 77, 79, **82**, **84**, **86**, 87, 119	127, 129, 130, **143**, 144, **145**, 146, 178, 217, 218, 245, 246, 248, 249, 250, 251

D

Sr. No.	Docking Platform	4A Interacting residues
		Receptor
1	PyDOCK	**E64, S65, H80, K81, Y82, C83, D84, P85, L89, V91, T101**
2	ZDOCK	**E64, S65, H80, K81, Y82, C83, D84, P85, L89,** R90, **V91,** K94, **T101**

Fig. 5. The docking of peptide (p-KGYY) with the CD40 receptor: A.) Diagrammatic representation of docking of the peptide with the CD40 receptor in PyDockWEB. 4 Å interacting residues are shown in a circle. **B.)** Diagrammatic representation of docking of the peptide with the CD40 receptor in ZDOCK. 4 Å interacting residues are shown in a circle. **C.)** 4 Å interacting residues in the crystal structure of CD40-CD40L (PDB 3QD6). **D.)** 4 Å interacting residues between the peptide and the receptor in PyDockWEB and ZDOCK. Similar residues in the docked structure and the crystal structure are highlighted in bold and critical residues on the receptor (82Y, 84, and 86N) are underlined. CD40 is highlighted in blue, and the peptide is highlighted in pink. (For interpretation of the references to colour in this figure legend, the reader is referred to the Web version of this article.)

Table 1
Physicochemical and ADMET analysis of peptide (p-KGYY).

Parameters		KGYY
Physiochemical parameters	**M.W. (Da)**	531.61
	LogP	−1.92
	Rotatable bond	15
	Acceptor bond	6
	Donor bond	8
Absorption	**Water Solubility (log mol/L)**	−3.086
	CaCo2 permeability (log Papp)	−0.26
	Intestinal absorption (in %)	6.574
	Skin permeability (logKp)	−2.735
Distribution	**Fraction unbound (Fu)**	0.39
	BBB permeability (logBB)	−0.692
	CNS permeability (logPS)	−4.368
Metabolism	**CYP2D6 substrate**	No
	CYP2D6 inhibitor	No
	CYP3A4 substrate	No
	CYP3A4 inhibitor	No
	CYP1A2 inhibitor	No
	CYP2C19 inhibitor	No
	CYP2C9 inhibitor	No
Excretion	**Total Clearance (log ml/min/kg)**	1.094
Toxicity	**AMES toxicity**	No
	Hepatotoxicity	Yes
	Skin sensitization	No

Water solubility (logS)- defines solubility in water at 25 °C; Skin permeability-logkp > − 2.5 classifies low skin permeability; Fraction unbound-defines unbound state in plasma protein remaining for pharmacological action; BBB permeability-logBB < − 1 classifies poorly distributed to the brain; CNS permeability-logPS > − 2 classifies CNS penetration and logPS < − 3 classifies no CNS penetration; Total clearance-includes both hepatic and renal clearance, Papp-apparent permeability coefficient. Da-dalton.

MMsMIMIC/) was used to derive the best peptidomimetic structures from the publicly available database. pep:MMs:MIMIC utilizes a 3D-similarity search of the peptide among 17 million available conformers of 3.9 million commercially available compounds in the MMsINC database (Masciocchi et al., 2009) and provides the top 200 molecules. The resultant molecules were individually docked to the CD40 receptor using AutoDock Vina (v1.2.0) (Eberhardt et al., 2021) and the Glide module of the Schrodinger suite (Friesner et al., 2004) and were then shortlisted based on their interaction with all the three critical residues (Y82, D84, and N86) on the CD40 receptor. One molecule (MMs01727545) was found to be interacting with all the three critical residues on CD40 along with the good docking score in both platforms (Fig. 6). However, the physicochemical and ADMET analyses still flagged a positive hepatotoxicity value for this compound (Table 2). Therefore, we next set out to search for the derivatives of our peptidomimetic structure (MMs01727545) with a comparable or greater binding affinity to CD40 and a negative hepatotoxicity value.

3.5. Designing the peptidomimetic derivatives and their docking to CD40

In this case, we utilized PubChem (https://pubchem.ncbi.nlm.nih.gov/) to identify the peptidomimetic derivatives. We performed a similarity search of the molecules by uploading SMILES ID of our lead peptidomimetic structure (MMs01727545) and downloading 1000 structurally identical molecules. The docking of these molecules was performed using AutoDock Vina (v1.2.0) (Trott and Olson, 2010) and Schrodinger Software (Friesner et al., 2004). Three molecules were identified (PubChem ID 121356761, 146599825, and 126700407) that were able to bind to all three critical residues of CD40 in both docking platforms (Fig. 7). Excitingly, the physicochemical and ADMET analyses of these molecules yielded negative hepatotoxicity values. In summary, these three derivatives interacted with all three critical residues on CD40 (Y82, D84, and N86), exhibited a higher binding affinity to CD40 as compared to the original peptidomimetic structure, and possessed good physicochemical and ADMET properties (Table 3).

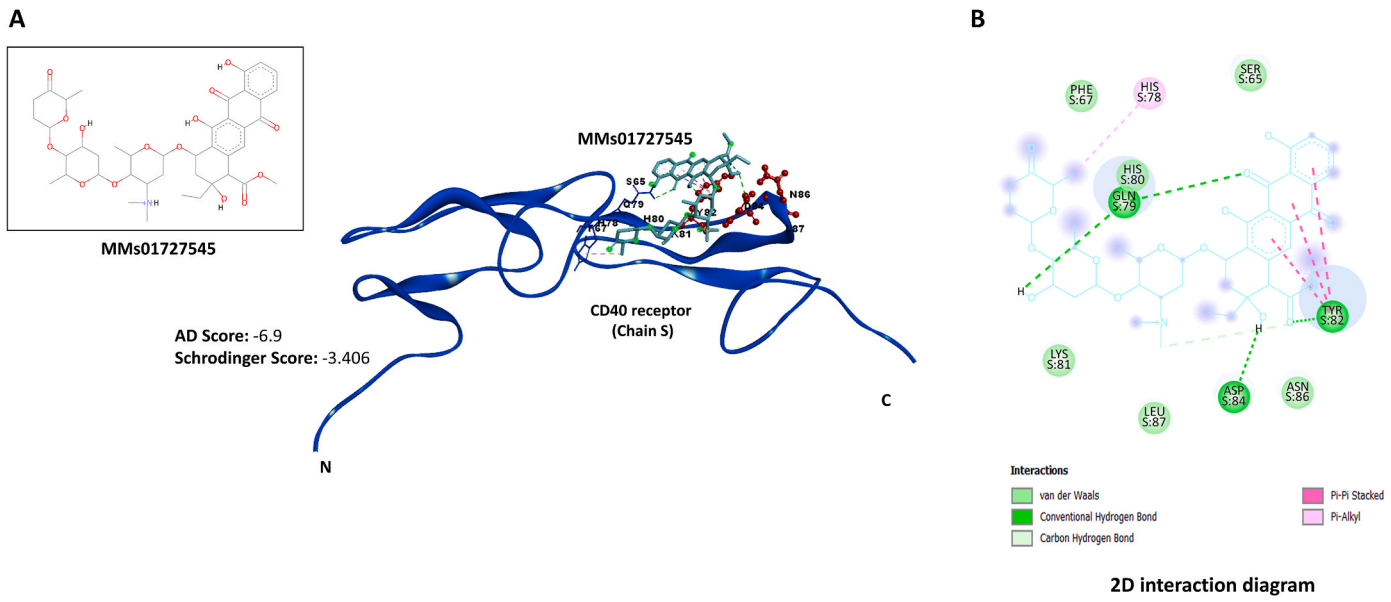

Fig. 6. The docking of peptidomimetic (MMs01727545) with the CD40 receptor: A.) Diagrammatic representation of the docking of the peptidomimetic (MMs01727545) with the CD40 receptor. Docking scores for AutoDock Vina and Schrodinger are indicated **B.)** 2D interaction diagram of the interacting residues between the receptor and the peptidomimetic structure (MMs01727545).

Table 2
Physicochemical and ADMET analysis of MMs01727545.

Parameters		MMs01727545
Physiochemical parameters	**M.W. (Da)**	812.8
	LogP	1.7
	Rotatable bond	9
	Acceptor bond	15
	Donor bond	5
Absorption	**Water Solubility (log mol/L)**	−3.073
	CaCo2 permeability (log Papp)	0.368
	Intestinal absorption (in %)	71.983
	Skin permeability (logKp)	−2.735
Distribution	**Fraction unbound (Fu)**	0.173
	BBB permeability (logBB)	−1.925
	CNS permeability (logPS)	−4.195
Metabolism	**CYP2D6 substrate**	No
	CYP2D6 inhibitor	No
	CYP3A4 substrate	Yes
	CYP3A4 inhibitor	No
	CYP1A2 inhibitor	No
	CYP2C19 inhibitor	No
	CYP2C9 inhibitor	No
Excretion	**Total Clearance (log ml/min/kg)**	1.274
Toxicity	**AMES toxicity**	No
	Hepatotoxicity	Yes
	Skin sensitization	No

Water solubility (logS)- defines solubility in water at 25 °C; Skin permeability-logkp > − 2.5 classifies low skin permeability; Fraction unbound-defines unbound state in plasma protein remaining for pharmacological action; BBB permeability-logBB < − 1 classifies poorly distributed to the brain; CNS permeability-logPS > − 2 classifies CNS penetration and logPS < − 3 classifies no CNS penetration; Total clearance-includes both hepatic and renal clearance, Papp-apparent permeability coefficient. Da-dalton.

3.6. Molecular dynamic simulation

Molecular dynamics simulation was carried out for period of 100 ns for all the apo and complex systems. Fig. S1 represents the RMSD of CD40R – CD40L and CD40R – Peptide complex systems with respect to the apo form. In Fig. S1, both receptor and ligand were stable, and the deviation is less than and equal to 3 Å which corresponds to smaller and globular conformational changes. In case of its complex system, the structure was stable till 30 ns, after that the RMSD gradually rises to 20 Å and reduces to 15 Å around 50 ns. The average RMSD was found to be 27.598 Å. The trajectory analysis indicates the loop region, and the terminal region of the receptor fluctuates more during the entire simulation with residues 119 to 122 and the receptor moves left and right with respect to the ligand. Similarly, in case of CD40R -peptide complex, the average RMSD was 11.499 Å and the complex deviates from its mean position throughout the simulation. Large RMSD value means that the peptide did not bound to the receptor in the binding pocket. Figs. S5 and S6 shows the superimposed image of complex structure. Fig. S2 depicts the RMSF of apo and complex systems. CD40L - CD40R complex has undergone very large structural changes. In case of CD40R – peptide complex, the residues present in the protein fluctuated much less than 1 nm, but the peptide fluctuates up to 4 nm around the system. Fig. S3 represents the radius of gyration (Rg) plot. In case of CD40R - CD40L system, the Rg values vary over the course of the simulation, indicating structural changes formed around 40 ns while peptide complex maintains the Rg value inferring compact and tight fold structure. Fig. S4 indicates that both complex structures have high solvent accessible surface area when compared to the apo form. Figs. S7–S10 shows the hydrogen bond contacts during the 100 ns simulation. CD40R – CD40L complex forms an average of 150 hydrogen bonds during the simulation time and CD40R – Peptide forms 80 hydrogen bonds at 20 ns.

4. Discussion

Computer-aided drug design approaches are powerful tools for drug discovery. In this study, we used these tools for *in silico* design of inhibitory peptides that could potentially disrupt the interaction between the CD40 receptor and CD40 ligand. The CD40-CD40L complex formation is implicated in the pathogenesis of atherosclerosis (Lacy et al., 2021). The CD40-CD40L interaction is critical during the rolling and adhesion of CD40 bearing monocytes on the CD40L positive endothelium, promoting monocytes extravasation and then transformation to macrophages that may later become foam cells after engulfing oxidized LDL (Lutgens et al., 2007). Macrophage accumulation in plaques causes atherosclerosis progression (Moore et al., 2013). Mechanistically, interaction of CD40 with the CD40L triggers the recruitment of Tumor necrosis factor receptor-associated factors (TRAFs) such as TRAF-2, -3, -5 and -6 (Lutgens et al., 2010). Interaction of CD40-TRAF6 has found to

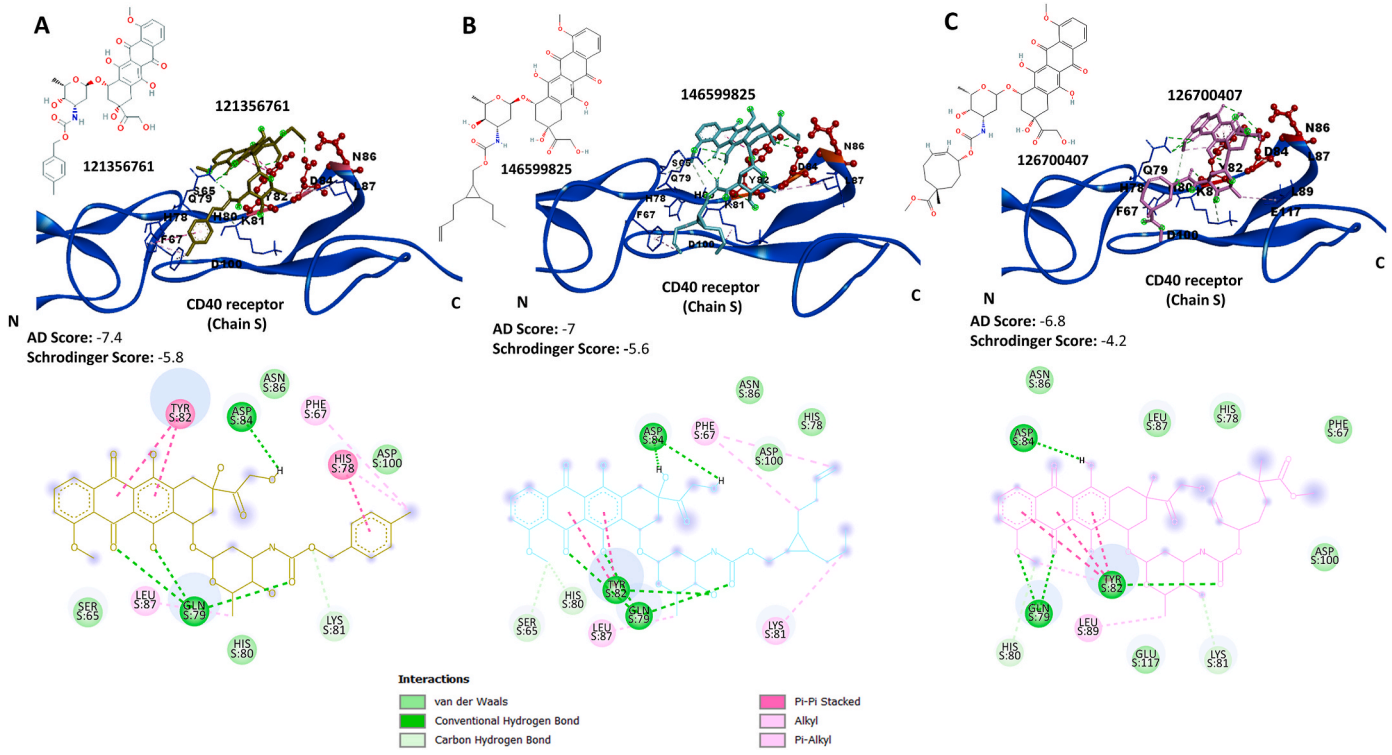

Fig. 7. The docking of the peptidomimetic derivatives with the CD40 receptor: Diagrammatic representation of the docking of individual peptidomimetic derivatives with the CD40 receptor in AutoDock Vina and Schrodinger along with the 2D interaction diagram. **A)** 121356761, **B)** 146599825, and **C)** 126700407. Individual docking scores have been indicated. Interacting residues between the complex have been highlighted. CD40 is highlighted in blue, and peptidomimetics are highlighted in pink. (For interpretation of the references to colour in this figure legend, the reader is referred to the Web version of this article.)

play an important role in plaque formation, while interaction with TRAF-2, -3 and -5 plays a minor role in the disease progression (Donners et al., 2008; Lutgens et al., 2010). Indeed, targeting CD40-TRAF6 interaction by TRAF-STOP inhibitor was found to attenuate the formation of atherosclerosis plaque in *Apoe*$^{-/-}$ mice (Seijkens et al., 2018). Atherosclerosis is a major CVD and a risk factor for myocardial infarction and stroke. Although lipid-lowering therapies, anti-hypertensive agents, and anti-platelets drugs are helpful in reducing the risk of CVD and save patient lives, novel alternative pharmacological tools are still needed. Thus, blocking CD40^{-}CD40L interactions with a targeted peptide would reduce macrophage accumulation in atherosclerotic lesions, and this may lead to the regression of atherosclerosis (Bosmans et al., 2021). The current study identified peptide and its peptidomimetic derivative which binds to the critical residues on the CD40 receptor involved in its interaction with the ligand and can block the receptor-ligand interaction, thus attenuating the disease progression.

4.1. The docking of the CD40 receptor to the CD40 ligand

The crystal structure of CD40-CD40L was downloaded from RCSB PDB (PDB 3QD6), and the monomeric chains of the CD40 receptor (Chain S) and CD40 ligand (Chain C) were studied to identify the interacting partners for each residue within the 4 Å range known to characterise ionic and hydrogen bonding in protein complexes. Analyses of the 4 Å residues between the complex is crucial as it dictates the involvement of critical residues involved in the interaction between the complex. We used UCSF Chimera (Pettersen et al., 2004) (Fig. 1; A and B) to perform this task. *In-vitro* mutational study established the critical role of residues Y82, D84, and N86 on CD40 and K143 and Y145 on CD40L in mediating the interaction within the protein-protein complex (Bajorath et al., 1995). Our analysis of the 4 Å interacting residues using the published crystal structure atomic coordinates also found the involvement of the same residues on the receptor as well as in the ligand, validating our computer modelling approach. We further validated our ability to identify critical residues in CD40 (Chain S) docked to CD40L (Chain C) by using PyDockWEB server (Jimenez-Garcia et al., 2013). PyDockWEB is a user-friendly server which allow the use of PyDOCK rigid-body protein-protein docking and scoring is performed based on electrostatics and desolvation energy (Cheng et al., 2007; Jimenez-Garcia et al., 2013). Again, the 4 Å interacting residues were successfully identified in the docked structure. We found the maximum similarity of residues between the docked and the crystal structure (Fig. 2), which further confirms the importance of these residues in mediating the receptor-ligand interaction.

4.2. The mutational analysis of CD40 and CD40L

After confirming *in silico* the importance of residues Y82, D84, and N86 on CD40 as well as K143 and Y145 residues on CD40L (Bajorath et al., 1995), we next aimed to perform the *in-silico* mutational analysis by replacing these critical residues with alanine which can impede the binding within the CD40-CD40L complex, resulting in the decrease in the binding affinity of CD40L to CD40. Replacement of critical residues using site-directed mutagenesis can help in deciphering the importance of that residue(s) in the interaction with the ligand. Alanine is the most common residue used as it is a simpler amino acid. Our result indeed indicated a decrease in the binding affinity of the receptor with the ligand in individually mutated complexes. The binding affinity was further decreased when the combined all three mutations were done in the CD40 receptor binding domain, further confirming the importance of these residues in the interaction with CD40L (Fig. 3). Vice versa, the replacement with alanine of the residues K143 and Y145 in the CD40L binding domain, individually or combined also resulted in a decrease in the binding affinity of the mutated CD40L to CD40 with a maximum decrease found when both residues were mutated simultaneously (Fig. 4). These results again confirmed the importance of the CD40L

Table 3
Summary of docking of peptidomimetics and their derivatives.

A.) Dock Scores and residual interaction of peptidomimetic (MMs01727545) and their derivatives (PubChem ID: 121356761, 146599825 and 126700407).

Parameters		MMs01727545	121356761	146599825	126700407
Dock Scores	Autodock Vina	−6.9	−7.4	−7	−6.8
	Interaction	82: h-bond, C–H bond; 84: h-bond; 86: VdW	82: pi-pi; 84: H-bond; 86: VdW	82: H-bond; pi-pi; 84: H-bond; 86: VdW	82: H-bond; pi-pi; 84: H-bond; 86: VdW
	Schrodinger	−3.406	−5.8	−5.6	−4.2
	Interaction	82: pi-pi; 84: h-bond; 86: VdW	82: H-bond; pi-pi; 84: H-bond; 86: VdW	82: H-bond; pi-pi; 84: H-bond; 86: VdW	82: H-bond; pi-pi; 84: H-bond; 86: VdW

B.) Comparison of physiochemical and ADMET properties of the peptide (p-KGYY), peptidomimetics and their derivatives.

Parameters		p-KGYY	MMs01727545	121356761	146599825	126700407
Physiochemical properties	**M.W. (Da)**	531.61	812.8	691.686	737.799	767.781
	LogP	−1.92	1.7	2.27742	3.3973	2.4469
	Rotatable bond	15	9	8	13	8
	Acceptor bond	6	15	13	13	15
	Donor bond	8	5	6	6	6
Absorption	**Water Solubility (log mol/L)**	−3.086	−3.073	−3.255	−3.392	−3.045
	CaCo2 permeability (log Papp)	−0.26	0.368	0.281	0.391	0.314
	Intestinal absorption (in %)	6.574	71.983	78.598	66.907	70.84
	Skin permeability (logKp)	−2.735	−2.735	−2.735	−2.735	−2.735
Distribution	**Fraction unbound (Fu)**	0.39	0.173	0	0.067	0.1
	BBB permeability (logBB)	−0.692	−1.925	−1.883	−1.826	−2.184
	CNS permeability (logPS)	−4.368	−4.195	−4.31	−4.052	−4.351
Metabolism	**CYP2D6 substrate**	No	No	No	No	No
	CYP2D6 inhibitor	No	No	No	No	No
	CYP3A4 substrate	No	Yes	Yes	Yes	Yes
	CYP3A4 inhibitor	No	No	No	No	No
	CYP1A2 inhibitor	No	No	No	No	No
	CYP2C19 inhibitor	No	No	No	No	No
	CYP2C9 inhibitor	No	No	No	No	No
Excretion	**Total Clearance (log ml/min/kg)**	1.094	1.274	−0.392	−0.13	−0.466
Toxicity	**AMES toxicity**	No	No	No	No	No
	Hepatotoxicity	Yes	Yes	No	No	No
	Skin sensitization	No	No	No	No	No

Water solubility (logS)- defines solubility in water at 25 °C; Skin permeability-logkp > -2.5 classifies low skin permeability; Fraction unbound-defines unbound state in plasma protein remaining for pharmacological action; BBB permeability-logBB < -1 classifies poorly distributed to the brain; CNS permeability-logPS > -2 classifies CNS penetration and logPS < -3 classifies no CNS penetration; Total clearance-includes both hepatic and renal clearance, Papp-apparent permeability coefficient. Da-dalton.

binding site residues for the interaction of the receptor and ligand, targeting which can help in the inhibition of the interaction between these two proteins.

4.3. Designing the blocking peptide and its docking to CD40

CD40L is important for the interaction of the immune cells and the platelets. Various cells involved in the plaque pathogenesis expresses CD40L on their surfaces (Mach et al., 1997). CD40L expression by cells such as T-cells and platelets plays an important role in their activation and disease progression (Michel et al., 2017). Also, CD40L present on the platelets plays a major role in the stabilization of thrombus (Andre et al., 2002). Notably, monoclonal antibody against CD40L has shown adverse side effects, such as thromboembolic events in humans and primates (Boumpas et al., 2003; Kawai et al., 2000). Therefore, in our study, we used the CD40 receptor as a therapeutic target. Another study has also targeted the CD40 receptor in atherosclerosis and found positive results in limiting the disease progression (Lutgens et al., 2010). Thus, a therapeutic peptide was designed against the CD40 receptor to limit its interaction with CD40L. Designing a therapeutic peptide is a well-known strategy to limit the protein-protein interaction (PPI) (Draeger and Mullen, 1994). Due to large and shallow interfaces of PPIs and the lack of binding pockets, PPIs is mostly regarded “undruggable” by small molecule inhibitors, while peptides designed against the critical residues involved in PPI serves as a good antagonist which can limit their interaction (Sillerud and Larson, 2005; Wang et al., 2021). Our peptides mimic the residues in the binding site of CD40, thus limiting the binding affinity of CD40L to CD40. Also, the usage of peptides as a therapeutics has several advantages over proteins or antibodies, such as low cost, lower toxicity, lower accumulation in tissues, high biological and chemical diversity, and high potency (Thundimadathil, 2012).

To identify the similarity of the involved residues between the docked structure of receptor-peptide complex and the crystal structure, the 4 Å interacting residues between the docked CD40 receptor-peptide (pKGYY) complex were analysed and compared with the interacting residues in the crystal structure. We found similarity in some of the interacting residues between the CD40 receptor-peptide (pKGYY) and the crystal structure of CD40-CD40L (Fig. 5). This result suggested that the peptide was interacting at the interface site of the receptor known for its interaction with the ligand and thus can limit the interaction of the receptor with the ligand. Therapeutic peptides have been successfully used as an antagonist for various cell-surface receptors (Wang et al., 2022). Although Y82 and D84 interacted with the p-KGYY, N86 was not involved in the interaction. To analyse the ADMET properties of the peptide, we used pkCSM server (Pires et al., 2015). pkCSM relies on the distance-based graph signature of the molecule to predict the pharmacokinetic and toxicity profiles. Many others studies have also reported the use of pkCSM for predicting the pharmacokinetics and toxicity profile of the molecule(s) (Abd El-Lateef et al., 2023; das Neves et al., 2023; Georgiou et al., 2023; Khamto et al., 2023; Presa et al., 2023). For ADMET analysis, following parameters where chosen. In absorption parameter, water solubility, CaCo2 permeability, intestinal absorption and skin permeability were considered. Water solubility reflects the solubility of the molecule in the water at 25 °C. Higher the negative value, better the solubility. CaCo2 permeability is used as an in-vitro model of human intestinal mucosa to predict the absorption of orally

administered drugs. $LogP_{app}$ greater than 0.9 suggest high CaCo2 permeability. Intestinal absorption predicts the percentage of compound absorbed through human intestine. Compound with value less than 30% considered poorly absorbed. Skin permeability predicts whether given compound is skin permeable for transdermal delivery. logKp >2.5 considered low skin permeable**.** In distribution parameter, fraction unbound, blood-brain barrier (BBB) permeability and central nervous system (CNS) permeability were considered. Fraction unbound predicts the fraction of the drug free from binding with the serum proteins. More the binding with the serum proteins, less efficiently it can diffuse. It predicts the value on scale of 0–1. BBB permeability is the ability of compound to cross the blood-brain barrier. logBB value above 0.3 is considered readily crossable, while value below −1 suggest poor distribution in brain. logPS value > −2 considered penetrable for CNS permeability while logPS < −3 considered impenetrable. In metabolism parameter, substrate and inhibitor for isoform of cytochrome P450 (CYP450) and total clearance were considered. Cytochrome P450 is a detoxifying enzyme in the liver which deactivates the drug. Cytochrome P450 substrate suggest whether the compound is substrate for CYP450 isoforms CYP2D6 and CYP3A4 for effective clearance. Cytochrome P450 inhibitor predicts whether compounds act as an inhibitor for isoforms of CYP450. Total clearance predicts the bioavailability of the drug and to suggest the dosing rates to achieve steady-state concentration. It combines hepatic and renal clearance. Positive value corresponds to high clearance. In toxicity parameter, Ames toxicity, hepatotoxicity and skin sensitization were considered. Ames Toxicity indicates the mutagenic potential of the compound. Positive value suggest compound is mutagenic and potential carcinogenic. Hepatotoxicity predicts whether the compound likely to associate with the disrupted normal functioning of the liver. Skin sensitization predicts whether the compound induce allergic contact dermatitis when encountered by skin. *In silico* physicochemical and ADMET analyses of the peptide revealed hepatotoxicity to be positive (Table 1). Hepatoxicity/Drug-induced liver injury (DILI) is one of the most frequent cause for the termination of drug development programs (David and Hamilton, 2010). Therefore, we further focused on the modifications of the parent peptide to improve its ADMET properties.

4.4. Peptidomimetic as a therapeutic strategy against CD40

There are several limitations associated with the natural peptides which limit their use, such as low oral bioavailability, short half-life, rapid clearance, and low metabolic stability, among others (Recio et al., 2016). We found that our designed peptide was not interacting with all the three critical residues in CD40 as well as the ADMET analysis predicted positive hepatotoxicity of the peptide. To address these drawbacks, peptidomimetics were used as a therapeutic option. Peptidomimetic has been sought as an improved therapeutic option compared to the peptide. Peptidomimetics mimics the original structure of the peptide with increased stability, improved target specificity, and good membrane permeability due to the addition of unnatural amino acids, backbone amide modification, and/or the addition of hydrophobic residues (Gentilucci et al., 2006; Vagner et al., 2008). Several reports had found improved outcomes when peptidomimetics were used as a therapeutic option (Ahmed et al., 2015; Amar et al., 2010; Chattopadhyay et al., 2013; Remaley et al., 2003). Peptidomimetics utilizes 3D conformations and pharmacophoric properties of the input peptide to provide resultant peptidomimetic structures present in the database. We used peptidomimetic server pep:MMs:MIMIC (http://mms.dsfarm.unipd.it/pepMMsMIMIC/) (Floris et al., 2011) to find the best peptidomimetic structures in the database. The resultant molecules were docked to CD40 in AutoDock Vina (v1.2.0) (Eberhardt et al., 2021) and Glide module of the Schrodinger suite (Friesner et al., 2004). After analysing the top 200 molecules, one molecule (MMs01727545) was found to be interacting with all three critical residues (Y82, D84, and N86) along with the good dock score in both platforms (Fig. 6). Further, physicochemical and ADMET properties of the compound were analysed in pkCSM server. The peptidomimetic MMs01727545 still showed positive hepatotoxicity (Table 2). Therefore, we resorted to identifying the derivatives of MMs01727545 which would preserve its backbone elements with slight modification in the side chains, that can increase the binding affinity of it to the receptor and may reduce the molecule hepatotoxicity.

We used PubChem server (https://pubchem.ncbi.nlm.nih.gov/) for conducting the similarity search of the parent peptidomimetic molecule using 3D conformers by uploading SMILES ID of the peptidomimetic structure (MMs01727545). This resulted in the identification of 1000 structurally identical molecules from the database. After docking these molecules using AutoDock Vina (v1.2.0) (Trott and Olson, 2010) and Schrodinger, we were able to narrow the number of hits to three molecules (PubChem ID 121356761, 146599825, and 126700407). These three modified peptidomimetics interacted with all three critical residues of CD40 in both docking platforms (Fig. 7). Interestingly, analysis of the ADMET properties of these molecules predicted no hepatotoxicity in pkCSM server (Table 3). In conclusion, our similarity search for the better modified peptidomimetics led us to the three best derivatives that were found to be interacting with the critical residues on CD40 receptor (Y82, D84, and N86) with higher binding affinity compared to the original peptidomimetic structure and had better physicochemical and ADMET properties compared to its counterpart (Table 3). Thus, we successfully identified peptidomimetics inhibitors capable of blocking the interaction between CD40 and CD40L. Such peptidomimetic inhibitors may potentially be useful for treating various autoimmune diseases such as atherosclerosis where CD40-40L interaction plays an important role in the progression of the disease.

4.5. Molecular dynamic simulation of CD40-40L and CD40-peptide

Molecular dynamics simulation was carried out for period of 100 ns for all the apo and complex systems. The MD results were evaluated to understand the conformational changes and structural deviations. For the analysis of macromolecular structures and their dynamic changes, the root-mean-square deviation (RMSD) stands out as a widely accepted measure of similarity. This examination helps us assess whether the simulation has reached a state of equilibrium and there were minimal disturbances towards the end of the simulation. It determines the change in selection of atom from a particular frame with respect to the reference frame. Fig. S5 represents the RMSD of CD40R – CD40L and CD40R – peptide complex systems with respect to apo form. In Fig. S1, ligand was stable, and the deviation is less than and equal to 3 Å which corresponds to smaller and globular conformational changes. The deviation of CD40R is > 3 Å in its apo form. In case of CD40R – CD40L complex system, the structure was stable till 30 ns, after that the RMSD gradually rises to 20 Å and reduces to 15 Å around 50 ns. The average RMSD was found to be 27.598 Å. The trajectory analysis indicates the loop region, and the terminal region of the receptor fluctuates more during the entire simulation with residues 119 to 122 and the receptor moves left and right with respect to the ligand. The trajectory movie has been attached as a supporting file. Similarly, in case of CD40R -peptide (p-KGYY) complex, the average RMSD was 11.499 Å and the complex deviates from its mean position throughout the simulation. From the trajectory analysis, it is seen that the peptide moves from its mean position to a larger extend. Based on the average RMSD value and the plot, it can be observed that the CD40R -peptide (p-KGYY) complex is relatively stable when compared to the CD40R - CD40L complex. Fig. S5 and S6 shows the superimposed image of complex structure. From the image (superimposed structure– green), the ligand (CD40L) and the receptor (CD40R) completely detached.

RMSF measures the variation or fluctuation in the positions of atoms over the course of an MD simulation. High RMSF values at specific regions of the molecule indicate that those areas are highly flexible and undergo significant fluctuations during the simulation. Conversely, low

RMSF values suggest rigidity or minimal atomic movements. Fig. S2 depicts the RMSF of apo and complex systems. CD40L - CD40R complex has undergone very large structural changes. All the residues present in the complex system has fluctuated more than 2 nm. In case of CD40R – peptide (p-KGYY) complex, the residues present in the protein fluctuated much less than 1 nm, but the peptide (p-KGYY) fluctuates up to 4 nm around the system.

Fig. S3 represents the radius of gyration plot which indicates the compactness of the protein. Smaller Rg values indicate a more compact and tightly folded structure, while larger Rg values suggest a more extended and less compact structure (Lobanov et al., 2008). In case of CD40R - CD40L system, the Rg values vary over the course of the simulation, indicating structural changes formed around 40 ns while peptide complex maintains the Rg value inferring compact and tight fold structure.

SASA, or solvent-accessible surface area, comes in handy during molecular dynamics (MD) simulations. It acts as our guide to discerning how much of a molecule's surface is available for interaction with the surrounding solvent molecules, offering valuable insights into the molecule's overall structure and behaviour. High SASA values imply that a larger portion of the molecule's surface is exposed to solvent, suggesting greater flexibility and conformational changes while low SASA values suggest that the molecule is more compact and buried within its own structure or is shielded from solvent molecules (Durham et al., 2009). Monitoring SASA can help identify conformational changes in proteins. Increased SASA may indicate the opening of a protein's binding pocket, while decreased SASA can signal pocket closure. With this context, from Fig. S4, it is seen that CD40R – CD40L complex has high solvent accessible surface area when compared to CD40R – peptide (p-KGYY) complex indicating peptide (p-KGYY) complex is more compact, less flexible, and secured from solvent molecules.

Figs. S3–S7 shows the hydrogen bond contacts during the 100 ns simulation. CD40R – CD40L complex forms an average of 150 hydrogen bonds during the simulation time and CD40R – peptide forms 80 hydrogen bonds at 20 ns. When comparing the H-bonds with respect to RMSD plot, interestingly, it is found that presence of more hydrogen bonds corresponds to stable and less deviating RMSD and vice versa. Based on the MD results, CD40R – CD40L complex had undergone very large conformation change when compared to the peptide complex. CD40R – CD40L complex has more access to the solvent which infers that the receptor is hydrophilic, and the peptide is more reactive in the complex structure.

5. Conclusion

The current study identified three compounds that can bind to the critical residues on the CD40 receptor and can potentially inhibit the interaction of CD40 and CD40L. The compounds possess good physicochemical and ADMET properties with higher binding affinity compared to the parent compound. Interaction of CD40 and CD40L is implicated in atherosclerosis progression. Based on the molecular dynamics analysis, the CD40-peptide complex is relatively stable than the CD40-CD40L complex based on RMSD, RMSF, radius of gyration, SASA, and H-bonds. Therefore, the designed molecule may potentially help reduce atherosclerosis. Although this *in-silico* study has its limitations, *in-vitro* testing of these compounds should be done to validate the computational findings.

Funding

This work was supported by Cumulative Professional Development Allowance (CPDA) and Research and Development Funds (RDF) from the Indian Institute of Technology Indore (IITI) to MSB. MSK acknowledges the generous support from the Research Supporting Project (RSP2023R352) by the King Saud University, Riyadh, Kingdom of Saudi Arabia. AGO was supported by a grant #NS102415 from the National Institutes of Health of the US.

CRediT authorship contribution statement

Kundan Solanki: Experiments, Writing – original draft. **Ashutosh Kumar:** Experiments, Writing – review & editing. **Mohd Shahnawaz Khan:** Experiments. **Subramani Karthikeyan:** Experiments. **Rajat Atre:** Experiments. **Kam Y.J. Zhang:** Writing – review & editing. **Evgeny Bezsonov:** Writing – review & editing. **Alexander G. Obukhov:** Writing – original draft, Writing – review & editing. **Mirza S. Baig:** Conceptualization, Investigation, Writing – original draft, Writing – review & editing, All authors have read and agreed to the published version of the manuscript.

Declaration of competing interest

The authors declare that they have no known competing financial interests or personal relationships that could have appeared to influence the work reported in this paper.

Data availability

Data will be made available on request.

Acknowledgments

The authors acknowledge the Indian Institute of Technology Indore (IITI) for providing facilities and other support. MSK acknowledges the generous support from the Research Supporting Project (RSP2023R352) by the King Saud University, Riyadh, Kingdom of Saudi Arabia. AGO acknowledges National Institutes of Health (NIH) USA for providing research grant (NS102415).

Appendix A. Supplementary data

Supplementary data to this article can be found online at https://doi.org/10.1016/j.crstbi.2023.100110.

References

Abd El-Lateef, H.M., Elmaaty, A.A., Abdel Ghany, L.M.A., Abdel-Aziz, M.S., Zaki, I., Ryad, N., 2023. Design and synthesis of 2-(4-Bromophenyl)Quinoline-4-carbohydrazide derivatives via molecular hybridization as novel microbial DNA-gyrase inhibitors. ACS Omega 8, 17948–17965. https://doi.org/10.1021/acsomega.3c01156.

Abraham, M.J., Murtola, T., Schulz, R., Páll, S., Smith, J.C., Hess, B., Lindahl, E.J.S., 2015. GROMACS: High Performance Molecular Simulations through Multi-Level Parallelism from Laptops to Supercomputers, vol. 1, pp. 19–25.

Aday, A.W., Ridker, P.M., 2019. Targeting residual inflammatory risk: a shifting paradigm for atherosclerotic disease. Front Cardiovasc Med 6, 16. https://doi.org/10.3389/fcvm.2019.00016.

Ahmed, C.M., Larkin 3rd, J., Johnson, H.M., 2015. SOCS1 mimetics and antagonists: a complementary approach to positive and negative regulation of immune function. Front. Immunol. 6, 183. https://doi.org/10.3389/fimmu.2015.00183.

Amar, M.J., D'Souza, W., Turner, S., Demosky, S., Sviridov, D., Stonik, J., Luchoomun, J., Voogt, J., Hellerstein, M., Sviridov, D., Remaley, A.T., 2010. 5A apolipoprotein mimetic peptide promotes cholesterol efflux and reduces atherosclerosis in mice. J. Pharmacol. Exp. Therapeut. 334, 634–641. https://doi.org/10.1124/jpet.110.167890.

An, H.J., Kim, Y.J., Song, D.H., Park, B.S., Kim, H.M., Lee, J.D., Paik, S.G., Lee, J.O., Lee, H., 2011. Crystallographic and mutational analysis of the CD40-CD154 complex and its implications for receptor activation. J. Biol. Chem. 286, 11226–11235. https://doi.org/10.1074/jbc.M110.208215.

Andre, P., Prasad, K.S., Denis, C.V., He, M., Papalia, J.M., Hynes, R.O., Phillips, D.R., Wagner, D.D., 2002. CD40L stabilizes arterial thrombi by a beta3 integrin–dependent mechanism. Nat. Med. 8, 247–252. https://doi.org/10.1038/nm0302-247.

Antosova, Z., Mackova, M., Kral, V., Macek, T., 2009. Therapeutic application of peptides and proteins: parenteral forever? Trends Biotechnol. 27, 628–635. https://doi.org/10.1016/j.tibtech.2009.07.009.

Audie, J., Boyd, C., 2010. The synergistic use of computation, chemistry and biology to discover novel peptide-based drugs: the time is right. Curr. Pharmaceut. Des. 16, 567–582. https://doi.org/10.2174/138161210790361425.

Bajorath, J., Chalupny, N.J., Marken, J.S., Siadak, A.W., Skonier, J., Gordon, M., Hollenbaugh, D., Noelle, R.J., Ochs, H.D., Aruffo, A., 1995. Identification of residues on CD40 and its ligand which are critical for the receptor-ligand interaction. Biochemistry 34, 1833–1844. https://doi.org/10.1021/bi00006a003.

Bosmans, L.A., Bosch, L., Kusters, P.J.H., Lutgens, E., Seijkens, T.T.P., 2021. The CD40-cd40l dyad as immunotherapeutic target in cardiovascular disease. J Cardiovasc Transl Res 14, 13–22. https://doi.org/10.1007/s12265-020-09994-3.

Boumpas, D.T., Furie, R., Manzi, S., Illei, G.G., Wallace, D.J., Balow, J.E., Vaishnaw, A., Group, B.G.L.N.T., 2003. A short course of BG9588 (anti-CD40 ligand antibody) improves serologic activity and decreases hematuria in patients with proliferative lupus glomerulonephritis. Arthritis Rheum. 48, 719–727. https://doi.org/10.1002/art.10856.

Chattopadhyay, A., Navab, M., Hough, G., Gao, F., Meriwether, D., Grijalva, V., Springstead, J.R., Palgnachari, M.N., Namiri-Kalantari, R., Su, F., Van Lenten, B.J., Wagner, A.C., Anantharamaiah, G.M., Farias-Eisner, R., Reddy, S.T., Fogelman, A. M., 2013. A novel approach to oral apoA-I mimetic therapy. J. Lipid Res. 54, 995–1010. https://doi.org/10.1194/jlr.M033555.

Cheng, T.M., Blundell, T.L., Fernandez-Recio, J., 2007. pyDock: electrostatics and desolvation for effective scoring of rigid-body protein-protein docking. Proteins 68, 503–515. https://doi.org/10.1002/prot.21419.

Croft, M., Benedict, C.A., Ware, C.F., 2013. Clinical targeting of the TNF and TNFR superfamilies. Nat. Rev. Drug Discov. 12, 147–168. https://doi.org/10.1038/nrd3930.

das Neves, A.R., Carvalho, D.B., Silva, F., Rosalem, R.F., Pelizaro, B.I., Castilho, P.F., Oliveira, K.M.P., Cassemiro, N.S., Pessatto, L.R., Paredes-Gamero, E.J., Piranda, E. M., Silva, D.B., Arruda, C.C.P., Baroni, A.C.M., 2023. In vivo antileishmanial effect of 3,5-Diaryl-isoxazole analogues based on veraguensin, grandisin, and machilin G: a glance at a preclinical study. ACS Infect. Dis. 9, 1150–1159. https://doi.org/10.1021/acsinfecdis.3c00090.

David, S., Hamilton, J.P., 2010. Drug-induced liver injury. US Gastroenterol Hepatol Rev 6, 73–80.

Donners, M.M., Beckers, L., Lievens, D., Munnix, I., Heemskerk, J., Janssen, B.J., Wijnands, E., Cleutjens, J., Zernecke, A., Weber, C., Ahonen, C.L., Benbow, U., Newby, A.C., Noelle, R.J., Daemen, M.J., Lutgens, E., 2008. The CD40-TRAF6 axis is the key regulator of the CD40/CD40L system in neointima formation and arterial remodeling. Blood 111, 4596–4604. https://doi.org/10.1182/blood-2007-05-088906.

Draeger, L.J., Mullen, G.P., 1994. Interaction of the bHLH-zip domain of c-Myc with H1-type peptides. Characterization of helicity in the H1 peptides by NMR. J. Biol. Chem. 269, 1785–1793.

Durham, E., Dorr, B., Woetzel, N., Staritzbichler, R., Meiler, J., 2009. Solvent accessible surface area approximations for rapid and accurate protein structure prediction. J. Mol. Model. 15, 1093–1108. https://doi.org/10.1007/s00894-009-0454-9.

Eberhardt, J., Santos-Martins, D., Tillack, A.F., Forli, S., 2021. AutoDock Vina 1.2.0: new docking methods, expanded force field, and Python bindings. J. Chem. Inf. Model. 61, 3891–3898. https://doi.org/10.1021/acs.jcim.1c00203.

Engel, D., Seijkens, T., Poggi, M., Sanati, M., Thevissen, L., Beckers, L., Wijnands, E., Lievens, D., Lutgens, E., 2009. The immunobiology of CD154-CD40-TRAF interactions in atherosclerosis. Semin. Immunol. 21, 308–312. https://doi.org/10.1016/j.smim.2009.06.004.

Floris, M., Masciocchi, J., Fanton, M., Moro, S., 2011. Swimming into peptidomimetic chemical space using pepMMsMIMIC. Nucleic Acids Res. 39, W261–W269. https://doi.org/10.1093/nar/gkr287.

Friesner, R.A., Banks, J.L., Murphy, R.B., Halgren, T.A., Klicic, J.J., Mainz, D.T., Repasky, M.P., Knoll, E.H., Shelley, M., Perry, J.K., Shaw, D.E., Francis, P., Shenkin, P.S., 2004. Glide: a new approach for rapid, accurate docking and scoring. 1. Method and assessment of docking accuracy. J. Med. Chem. 47, 1739–1749. https://doi.org/10.1021/jm0306430.

Gao, Y., Lee, J., Smith, I.P.S., Lee, H., Kim, S., Qi, Y., Klauda, J.B., Widmalm, G., Khalid, S., Im, W., 2021. CHARMM-GUI supports hydrogen mass repartitioning and different protonation states of phosphates in lipopolysaccharides. J. Chem. Inf. Model. 61, 831–839. https://doi.org/10.1021/acs.jcim.0c01360.

Gentilucci, L., Tolomelli, A., Squassabia, F., 2006. Peptides and peptidomimetics in medicine, surgery and biotechnology. Curr. Med. Chem. 13, 2449–2466. https://doi.org/10.2174/092986706777935041.

Georgiou, N., Chontzopoulou, E., Cheilari, A., Katsogiannou, A., Karta, D., Vavougyiou, K., Hadjipavlou-Litina, D., Javornik, U., Plavec, J., Tzeli, D., Vassiliou, S., Mavromoustakos, T., 2023. Thiocarbohydrazone and chalcone-derived 3,4-dihydropyrimidinethione as lipid peroxidation and soybean lipoxygenase inhibitors. ACS Omega 8, 11966–11977. https://doi.org/10.1021/acsomega.2c07625.

Jimenez-Garcia, B., Pons, C., Fernandez-Recio, J., 2013. pyDockWEB: a web server for rigid-body protein-protein docking using electrostatics and desolvation scoring. Bioinformatics 29, 1698–1699. https://doi.org/10.1093/bioinformatics/btt262.

Jo, S., Kim, T., Iyer, V.G., Im, W., 2008. CHARMM-GUI: a web-based graphical user interface for CHARMM. J. Comput. Chem. 29, 1859–1865. https://doi.org/10.1002/jcc.20945.

Kawai, T., Andrews, D., Colvin, R.B., Sachs, D.H., Cosimi, A.B., 2000. Thromboembolic complications after treatment with monoclonal antibody against CD40 ligand. Nat. Med. 6, 114. https://doi.org/10.1038/72162.

Khamto, N., Utama, K., Tateing, S., Sangthong, P., Rithchumpon, P., Cheechana, N., Saiai, A., Semakul, N., Punyodom, W., Meepowpan, P., 2023. Discovery of natural bisbenzylisoquinoline analogs from the library of Thai traditional plants as SARS-CoV-2 3CL(pro) inhibitors: in silico molecular docking, molecular dynamics, and in vitro enzymatic activity. J. Chem. Inf. Model. 63, 2104–2121. https://doi.org/10.1021/acs.jcim.2c01309.

Kotowicz, K., Dixon, G.L., Klein, N.J., Peters, M.J., Callard, R.E., 2000. Biological function of CD40 on human endothelial cells: costimulation with CD40 ligand and interleukin-4 selectively induces expression of vascular cell adhesion molecule-1 and P-selectin resulting in preferential adhesion of lymphocytes. Immunology 100, 441–448. https://doi.org/10.1046/j.1365-2567.2000.00061.x.

Kusters, P.J.H., Lutgens, E., Seijkens, T.T.P., 2018. Exploring immune checkpoints as potential therapeutic targets in atherosclerosis. Cardiovasc. Res. 114, 368–377. https://doi.org/10.1093/cvr/cvx248.

Lacy, M., Burger, C., Shami, A., Ahmadsei, M., Winkels, H., Nitz, K., van Tiel, C.M., Seijkens, T.T.P., Kusters, P.J.H., Karshovka, E., Prange, K.H.M., Wu, Y., Brouns, S.L. N., Unterlugauer, S., Kuijpers, M.J.E., Reiche, M.E., Steffens, S., Edsfeldt, A., Megens, R.T.A., Heemskerk, J.W.M., Goncalves, I., Weber, C., Gerdes, N., Atzler, D., Lutgens, E., 2021. Cell-specific and divergent roles of the CD40L-CD40 axis in atherosclerotic vascular disease. Nat. Commun. 12, 3754. https://doi.org/10.1038/s41467-021-23909-z.

Leader, B., Baca, Q.J., Golan, D.E., 2008. Protein therapeutics: a summary and pharmacological classification. Nat. Rev. Drug Discov. 7, 21–39. https://doi.org/10.1038/nrd2399.

Lee, J., Cheng, X., Swails, J.M., Yeom, M.S., Eastman, P.K., Lemkul, J.A., Wei, S., Buckner, J., Jeong, J.C., Qi, Y., Jo, S., Pande, V.S., Case, D.A., Brooks 3rd, C.L., MacKerell Jr., A.D., Klauda, J.B., Im, W., 2016. CHARMM-GUI input generator for NAMD, GROMACS, AMBER, OpenMM, and CHARMM/OpenMM simulations using the CHARMM36 additive force field. J. Chem. Theor. Comput. 12, 405–413. https://doi.org/10.1021/acs.jctc.5b00935.

Li Petri, G., Di Martino, S., De Rosa, M., 2022. Peptidomimetics: an overview of recent medicinal chemistry efforts toward the discovery of novel small molecule inhibitors. J. Med. Chem. 65, 7438–7475. https://doi.org/10.1021/acs.jmedchem.2c00123.

Lobanov, M., Bogatyreva, N.S., Galzitskaia, O.V., 2008. [Radius of gyration is indicator of compactness of protein structure]. Mol Biol (Mosk) 42, 701–706.

Lu, C., Wu, C., Ghoreishi, D., Chen, W., Wang, L., Damm, W., Ross, G.A., Dahlgren, M.K., Russell, E., Von Bargen, C.D., Abel, R., Friesner, R.A., Harder, E.D., 2021. OPLS4: improving force field accuracy on challenging regimes of chemical space. J. Chem. Theor. Comput. 17, 4291–4300. https://doi.org/10.1021/acs.jctc.1c00302.

Lusis, A.J., 2000. Atherosclerosis. Nature 407, 233–241. https://doi.org/10.1038/35025203.

Lutgens, E., Lievens, D., Beckers, L., Donners, M., Daemen, M., 2007. CD40 and its ligand in atherosclerosis. Trends Cardiovasc. Med. 17, 118–123. https://doi.org/10.1016/j.tcm.2007.02.004.

Lutgens, E., Cleutjens, K.B., Heeneman, S., Koteliansky, V.E., Burkly, L.C., Daemen, M.J., 2000. Both early and delayed anti-CD40L antibody treatment induces a stable plaque phenotype. Proc. Natl. Acad. Sci. U. S. A. 97, 7464–7469. https://doi.org/10.1073/pnas.97.13.7464.

Lutgens, E., Lievens, D., Beckers, L., Wijnands, E., Soehnlein, O., Zernecke, A., Seijkens, T., Engel, D., Cleutjens, J., Keller, A.M., Naik, S.H., Boon, L., Oufella, H.A., Mallat, Z., Ahonen, C.L., Noelle, R.J., de Winther, M.P., Daemen, M.J., Biessen, E.A., Weber, C., 2010. Deficient CD40-TRAF6 signaling in leukocytes prevents atherosclerosis by skewing the immune response toward an antiinflammatory profile. J. Exp. Med. 207, 391–404. https://doi.org/10.1084/jem.20091293.

Mach, F., Schonbeck, U., Sukhova, G.K., Bourcier, T., Bonnefoy, J.Y., Pober, J.S., Libby, P., 1997. Functional CD40 ligand is expressed on human vascular endothelial cells, smooth muscle cells, and macrophages: implications for CD40-CD40 ligand signaling in atherosclerosis. Proc. Natl. Acad. Sci. U. S. A. 94, 1931–1936. https://doi.org/10.1073/pnas.94.5.1931.

MacKerell Jr., A.D., Banavali, N., Foloppe, N., 2000. Development and current status of the CHARMM force field for nucleic acids. Biopolymers: original Research on biomolecules 56, 257–265.

Maier, J.A., Martinez, C., Kasavajhala, K., Wickstrom, L., Hauser, K.E., Simmerling, C., 2015. ff14SB: improving the accuracy of protein side chain and backbone parameters from ff99SB. J. Chem. Theor. Comput. 11, 3696–3713. https://doi.org/10.1021/acs.jctc.5b00255.

Masciocchi, J., Frau, G., Fanton, M., Sturlese, M., Floris, M., Pireddu, L., Palla, P., Cedrati, F., Rodriguez-Tome, P., Moro, S., 2009. MMsINC: a large-scale chemoinformatics database. Nucleic Acids Res. 37, D284–D290. https://doi.org/10.1093/nar/gkn727.

Michel, N.A., Zirlik, A., Wolf, D., 2017. CD40L and its receptors in atherothrombosis-an update. Front Cardiovasc Med 4, 40. https://doi.org/10.3389/fcvm.2017.00040.

Moore, K.J., Sheedy, F.J., Fisher, E.A., 2013. Macrophages in atherosclerosis: a dynamic balance. Nat. Rev. Immunol. 13, 709–721. https://doi.org/10.1038/nri3520.

Morris, G.M., Huey, R., Lindstrom, W., Sanner, M.F., Belew, R.K., Goodsell, D.S., Olson, A.J., 2009. AutoDock4 and AutoDockTools4: automated docking with selective receptor flexibility. J. Comput. Chem. 30, 2785–2791. https://doi.org/10.1002/jcc.21256.

O'Boyle, N.M., Banck, M., James, C.A., Morley, C., Vandermeersch, T., Hutchison, G.R., 2011. Open Babel: an open chemical toolbox. J. Cheminf. 3, 33. https://doi.org/10.1186/1758-2946-3-33.

Olsson, M.H., Sondergaard, C.R., Rostkowski, M., Jensen, J.H., 2011. PROPKA3: consistent treatment of internal and surface residues in empirical pKa predictions. J. Chem. Theor. Comput. 7, 525–537. https://doi.org/10.1021/ct100578z.

Peikert, A., Kaier, K., Merz, J., Manhart, L., Schafer, I., Hilgendorf, I., Hehn, P., Wolf, D., Willecke, F., Sheng, X., Clemens, A., Zehender, M., von Zur Muhlen, C., Bode, C., Zirlik, A., Stachon, P., 2020. Residual inflammatory risk in coronary heart disease: incidence of elevated high-sensitive CRP in a real-world cohort. Clin. Res. Cardiol. 109, 315–323. https://doi.org/10.1007/s00392-019-01511-0.

Pettersen, E.F., Goddard, T.D., Huang, C.C., Couch, G.S., Greenblatt, D.M., Meng, E.C., Ferrin, T.E., 2004. UCSF Chimera–a visualization system for exploratory research and analysis. J. Comput. Chem. 25, 1605–1612. https://doi.org/10.1002/jcc.20084.

Pierce, B.G., Wiehe, K., Hwang, H., Kim, B.H., Vreven, T., Weng, Z., 2014. ZDOCK server: interactive docking prediction of protein-protein complexes and symmetric multimers. Bioinformatics 30, 1771–1773. https://doi.org/10.1093/bioinformatics/btu097.

Pires, D.E., Blundell, T.L., Ascher, D.B., 2015. pkCSM: predicting small-molecule pharmacokinetic and toxicity properties using graph-based signatures. J. Med. Chem. 58, 4066–4072. https://doi.org/10.1021/acs.jmedchem.5b00104.

Presa, M.H., Rocha, M.J.D., Pires, C.S., Ledebuhr, K.N.B., Costa, G.P.D., Alves, D., Bortolatto, C.F., Bruning, C.A., 2023. Antidepressant-like effect of 1-(2-(4-(4-ethylphenyl)-1H-1,2,3-triazol-1-yl)phenyl)ethan-1-one in mice: evidence of the contribution of the serotonergic system. ACS Chem. Neurosci. 14, 2333–2346. https://doi.org/10.1021/acschemneuro.3c00108.

Quezada, S.A., Jarvinen, L.Z., Lind, E.F., Noelle, R.J., 2004. CD40/CD154 interactions at the interface of tolerance and immunity. Annu. Rev. Immunol. 22, 307–328. https://doi.org/10.1146/annurev.immunol.22.012703.104533.

Recio, C., Maione, F., Iqbal, A.J., Mascolo, N., De Feo, V., 2016. The potential therapeutic application of peptides and peptidomimetics in cardiovascular disease. Front. Pharmacol. 7, 526. https://doi.org/10.3389/fphar.2016.00526.

Remaley, A.T., Thomas, F., Stonik, J.A., Demosky, S.J., Bark, S.E., Neufeld, E.B., Bocharov, A.V., Vishnyakova, T.G., Patterson, A.P., Eggerman, T.L., Santamarina-Fojo, S., Brewer, H.B., 2003. Synthetic amphipathic helical peptides promote lipid efflux from cells by an ABCA1-dependent and an ABCA1-independent pathway. J. Lipid Res. 44, 828–836. https://doi.org/10.1194/jlr.M200475-JLR200.

Ridker, P.M., Everett, B.M., Pradhan, A., MacFadyen, J.G., Solomon, D.H., Zaharris, E., Mam, V., Hasan, A., Rosenberg, Y., Iturriaga, E., Gupta, M., Tsigoulis, M., Verma, S., Clearfield, M., Libby, P., Goldhaber, S.Z., Seagle, R., Ofori, C., Saklayen, M., Butman, S., Singh, N., Le May, M., Bertrand, O., Johnston, J., Paynter, N.P., Glynn, R.J., Investigators, C., 2019. Low-dose methotrexate for the prevention of atherosclerotic events. N. Engl. J. Med. 380, 752–762. https://doi.org/10.1056/NEJMoa1809798.

Ridker, P.M., Everett, B.M., Thuren, T., MacFadyen, J.G., Chang, W.H., Ballantyne, C., Fonseca, F., Nicolau, J., Koenig, W., Anker, S.D., Kastelein, J.J.P., Cornel, J.H., Pais, P., Pella, D., Genest, J., Cifkova, R., Lorenzatti, A., Forster, T., Kobalava, Z., Vida-Simiti, L., Flather, M., Shimokawa, H., Ogawa, H., Dellborg, M., Rossi, P.R.F., Troquay, R.P.T., Libby, P., Glynn, R.J., Group, C.T., 2017. Antiinflammatory therapy with canakinumab for atherosclerotic disease. N. Engl. J. Med. 377, 1119–1131. https://doi.org/10.1056/NEJMoa1707914.

Roy, A., Saqib, U., Baig, M.S., 2021. NOS1-mediated macrophage and endothelial cell interaction in the progression of atherosclerosis. Cell Biol. Int. 45, 1191–1201. https://doi.org/10.1002/cbin.11558.

Sastry, G.M., Adzhigirey, M., Day, T., Annabhimoju, R., Sherman, W., 2013. Protein and ligand preparation: parameters, protocols, and influence on virtual screening enrichments. J. Comput. Aided Mol. Des. 27, 221–234. https://doi.org/10.1007/s10822-013-9644-8.

Schonbeck, U., Mach, F., Sukhova, G.K., Herman, M., Graber, P., Kehry, M.R., Libby, P., 2000. CD40 ligation induces tissue factor expression in human vascular smooth muscle cells. Am. J. Pathol. 156, 7–14. https://doi.org/10.1016/S0002-9440(10)64699-8.

Schrodinger, 2021a. Schrodinger Release 2021-2. Ligprep, New York, NY.

Schrodinger, 2021b. Schrodinger Release 2021-2: Protein Preparation Wizard.

Seijkens, T.T.P., van Tiel, C.M., Kusters, P.J.H., Atzler, D., Soehnlein, O., Zarzycka, B., Aarts, S., Lameijer, M., Gijbels, M.J., Beckers, L., den Toom, M., Slutter, B., Kuiper, J., Duchene, J., Aslani, M., Megens, R.T.A., van 't Veer, C., Kooij, G., Schrijver, R., Hoeksema, M.A., Boon, L., Fay, F., Tang, J., Baxter, S., Jongejan, A., Moerland, P.D., Vriend, G., Bleijlevens, B., Fisher, E.A., Duivenvoorden, R., Gerdes, N., de Winther, M.P.J., Nicolaes, G.A., Mulder, W.J.M., Weber, C., Lutgens, E., 2018. Targeting CD40-Induced TRAF6 Signaling in Macrophages Reduces Atherosclerosis. J Am Coll Cardiol 71, 527–542. https://doi.org/10.1016/j.jacc.2017.11.055.

Seo, P.J., Hong, S.-Y., Kim, S.-G., Park, C.M., 2011. Competitive inhibition of transcription factors by small interfering peptides. Trends Plant Sci 16, 541–549.

Sillerud, L.O., Larson, R.S., 2005. Design and structure of peptide and peptidomimetic antagonists of protein-protein interaction. Curr. Protein Pept. Sci. 6, 151–169. https://doi.org/10.2174/1389203053545462.

Tardif, J.C., Kouz, S., Waters, D.D., Bertrand, O.F., Diaz, R., Maggioni, A.P., Pinto, F.J., Ibrahim, R., Gamra, H., Kiwan, G.S., Berry, C., Lopez-Sendon, J., Ostadal, P., Koenig, W., Angoulvant, D., Gregoire, J.C., Lavoie, M.A., Dube, M.P., Rhainds, D., Provencher, M., Blondeau, L., Orfanos, A., L'Allier, P.L., Guertin, M.C., Roubille, F., 2019. Efficacy and safety of low-dose colchicine after myocardial infarction. N. Engl. J. Med. 381, 2497–2505. https://doi.org/10.1056/NEJMoa1912388.

Thundimadathil, J., 2012. Cancer treatment using peptides: current therapies and future prospects. J. Amino Acids, 967347. https://doi.org/10.1155/2012/967347, 2012.

Timmerman, P., Beld, J., Puijk, W.C., Meloen, R.H., 2005. Rapid and quantitative cyclization of multiple peptide loops onto synthetic scaffolds for structural mimicry of protein surfaces. Chembiochem 6, 821–824. https://doi.org/10.1002/cbic.200400374.

Trott, O., Olson, A.J., 2010. AutoDock Vina: improving the speed and accuracy of docking with a new scoring function, efficient optimization, and multithreading. J. Comput. Chem. 31, 455–461. https://doi.org/10.1002/jcc.21334.

Vagner, J., Qu, H., Hruby, V.J., 2008. Peptidomimetics, a synthetic tool of drug discovery. Curr. Opin. Chem. Biol. 12, 292–296. https://doi.org/10.1016/j.cbpa.2008.03.009.

Van Der Spoel, D., Lindahl, E., Hess, B., Groenhof, G., Mark, A.E., Berendsen, H.J., 2005. GROMACS: fast, flexible, and free. J. Comput. Chem. 26, 1701–1718. https://doi.org/10.1002/jcc.20291.

Vanommeslaeghe, K., Hatcher, E., Acharya, C., Kundu, S., Zhong, S., Shim, J., Darian, E., Guvench, O., Lopes, P., Vorobyov, I., Mackerell Jr., A.D., 2010. CHARMM general force field: a force field for drug-like molecules compatible with the CHARMM all-atom additive biological force fields. J. Comput. Chem. 31, 671–690. https://doi.org/10.1002/jcc.21367.

Wang, L., Wang, N., Zhang, W., Cheng, X., Yan, Z., Shao, G., Wang, X., Wang, R., Fu, C., 2022. Therapeutic peptides: current applications and future directions. Signal Transduct. Targeted Ther. 7, 48. https://doi.org/10.1038/s41392-022-00904-4.

Wang, X., Ni, D., Liu, Y., Lu, S., 2021. Rational design of peptide-based inhibitors disrupting protein-protein interactions. Front. Chem. 9, 682675 https://doi.org/10.3389/fchem.2021.682675.

Yan, Y., Tao, H., He, J., Huang, S.Y., 2020. The HDOCK server for integrated protein-protein docking. Nat. Protoc. 15, 1829–1852. https://doi.org/10.1038/s41596-020-0312-x.